J. exp. Biol. **162**, 131–155 (1992)
Printed in Great Britain © *The Company of Biologists Limited 1992*

STIFFNESS AND DAMPING FORCES IN THE INTERVERTEBRAL JOINTS OF BLUE MARLIN (*MAKAIRA NIGRICANS*)

BY JOHN H. LONG, JR*

Department of Zoology, Duke University, Durham, NC 27706, USA and *Pacific Ocean Research Foundation, 74-425 Kealakehe Pkwy 15, Kailua-Kona, HI 96740, USA*

Accepted 9 September 1991

Summary

The stiffness and damping moments that are transmitted by intervertebral joints during sinusoidal bending were determined in the blue marlin, *Makaira nigricans* Lacépède. Using a dynamic bending machine, the angular stiffness ($N\,m\,rad^{-1}$) and damping coefficient ($kg\,m^2\,rad^{-2}\,s^{-1}$) of the intervertebral joints were measured over a range of bending frequencies, amplitudes and positions along the backbone. Angular stiffness increases with increasing bending amplitude, but, for some joints, the rate at which it changes with increasing bending frequency is negative. The precaudal intervertebral joints are less stiff than the caudal joints. The damping coefficient, which also shows regional variation, does not change with amplitude but does decrease with increasing bending frequency in joint positions three and five. Stiffness moments along the vertebral column, given the same amount of bending at each joint, are always greater than the damping moments. However, damping moments increase by an order of magnitude with an increase in bending frequency from 0.5 to 5.0 Hz. The stiffness and damping moments determine the work that an external moment, such as muscle, must do over a complete cycle of bending. The external moments and work needed to bend an intervertebral joint are determined largely by the stiffness moments of the intervertebral joints.

Introduction

Because the vertebrate body is mechanically complex, recent attempts to measure and model the transmission of muscular force and power in swimming fishes have remained incomplete (Hess and Videler, 1984; Johnsrude and Webb, 1985; Van Leewen *et al.* 1990). For example, while up to 94 % of muscle force may be lost in transmission to the tail (Johnsrude and Webb, 1985), the contribution of individual structures is still unknown (Van Leewen *et al.* 1990). One structure

* Present address: Department of Biology, Vassar College, Poughkeepsie, NY 12601, USA.

Key words: intervertebral joints, *Makaira nigricans*, force transmission, stiffness, damping, blue marlin, dynamic bending.

often implicated in force transmission – because of its connections to the lateral musculature, its axial position and its varied morphology – is the backbone (Home, 1809; Gregory and Conrad, 1937; Rockwell *et al.* 1938; Symmons, 1979; Wainwright, 1983).

Unfortunately, the forces transmitted by the backbone during swimming cannot be modeled from existing descriptions of the mechanical properties of fish backbones. This is because mechanical tests of the backbones of Norfolk spot *Leiostomus xanthurus*, skipjack tuna *Katsuwonus pelamis* (Hebrank, 1982) and blue marlin *Makaira nigricans* (Hebrank *et al.* 1990) were quasi-static, that is without specific reference to bending rate. Since the rate at which biological materials are deformed may drastically alter their mechanical properties (Wainwright *et al.* 1976), the mechanical function of the backbone over the range of tailbeat frequencies that occur during swimming can only be understood using mechanical properties that are measured dynamically. Therefore, the goals of this study are (1) to determine the force-transmitting capabilities of the backbone when tested at *in vivo* bending rates, (2) to determine whether the mechanical properties of the backbone vary with changes in bending amplitude, frequency and position along the axis, and (3) to describe how the mechanical properties are correlated with vertebral morphology.

Intervertebral joints

This mechanical study focuses on the intervertebral joints, which, because of their relative flexibility compared to the vertebral centra, have been proposed as functionally important structures in the bending backbone (Home, 1809). The backbone I have chosen, because of its extremely robust structure (Cuvier and Valenciennes, 1831), is the vertebral column of the blue marlin *Makaira nigricans*. Each of the 23 intervertebral joints consists of intervertebral ligaments, which make up the biconic capsule connecting the centra (for teleosts in general see Symmons, 1979), as well as the large overlapping processes of the vertebrae (zygapophyses, neural and hemal spines) and their fibrous interconnections. Like all species of the family Istiophoridae, the neural and hemal spines have been modified into large, flat, thin plates that overlap the intervertebral joint and interlock *via* fibrous connective tissues with the expanded zygapophyses (Fig. 1).

This spectacular vertebral morphology has suggested a potential spring-like function to previous investigators (Gregory and Conrad, 1937; Rockwell *et al.* 1938; Hebrank *et al.* 1990). A spring transmits a force that is proportional to its change of shape or deformation. However, in addition to spring forces, even simple mechanical systems in motion also have damping forces, which retard motion, and inertial forces, which act in opposition to spring forces.

Mechanical properties

In order to describe the relationship between externally applied forces and the resulting motions in intervertebral joints, I employ the analytical methods of vibratory mechanics (Den Hartog, 1956). As a first approximation, each interver-

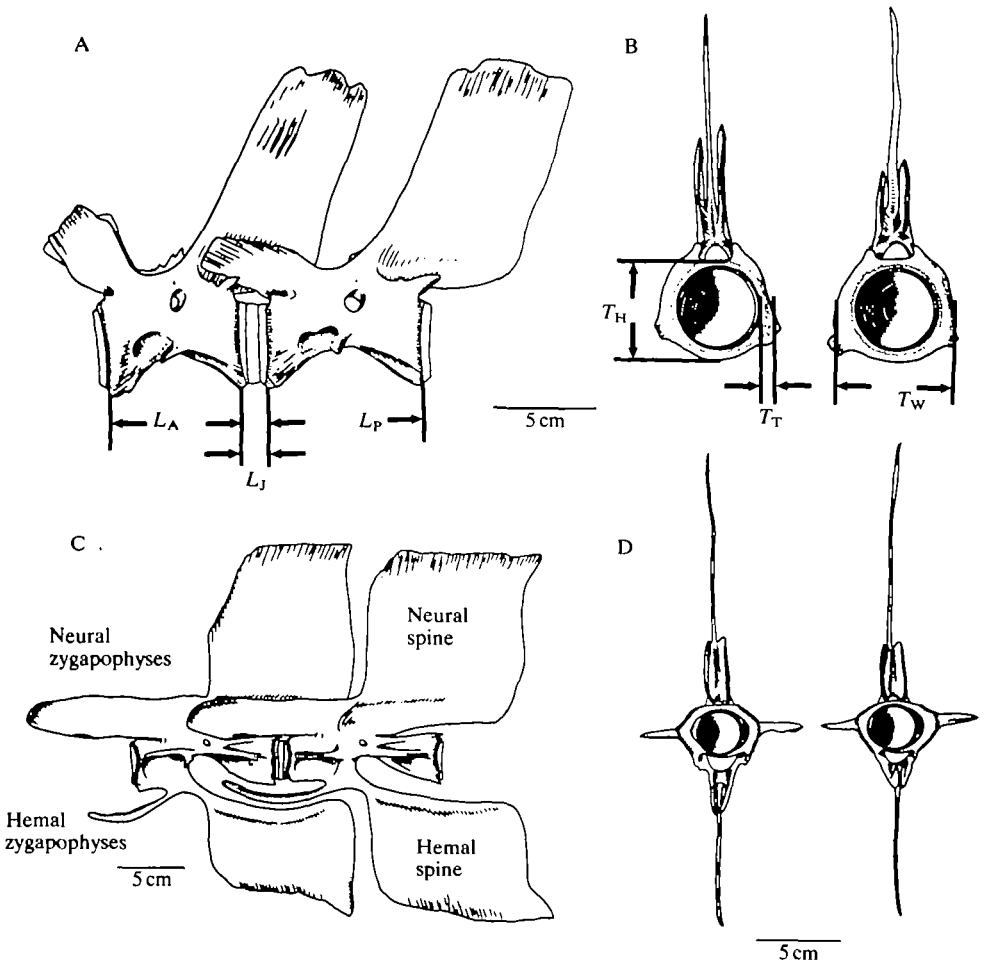

Fig. 1. Vertebrae and intervertebral joints of blue marlin showing morphological characters measured. (A) Two precaudal vertebrae, left lateral view. (B) Two precaudal vertebrae, anterior view. (C) Two caudal vertebrae, left lateral view. (D) Two caudal vertebrae, anterior view. Scale bars are 5 cm and illustrations are drawn to different scales. The morphological characters were length of vertebral centra anterior and posterior to the joint, L_A and L_P, length of intervertebral ligaments, L_J, transverse height and width of the intervertebral capsule, T_H and T_W, and transverse lateral thickness of the intervertebral capsule, T_T.

tebral joint is treated as a sinusoidally bending, single-degree-of-freedom system. This approximation assumes that the bending motion of an intervertebral joint can be described with one variable, the angular position, θ, in radians. By forcing an intervertebral joint to bend laterally back and forth with a maximum angular displacement, θ_0, at a given angular frequency, ω, in radians per second, I can

measure the bending force causing the bending motion as a dynamic bending moment (force times a moment arm) (from equation 2.2 of Den Hartog, 1956):

$$M_0\sin(\omega t) = k\theta_0\sin(\omega t - \delta) + c\theta_0\omega\cos(\omega t - \delta) - I\theta_0\omega^2\sin(\omega t - \delta), \quad (1)$$

which can also be stated in words as:

$$\begin{matrix}\text{bending} \\ \text{moment}\end{matrix} = \begin{matrix}\text{moment due to} \\ \text{stiffness}\end{matrix} + \begin{matrix}\text{moment due to} \\ \text{damping}\end{matrix} - \begin{matrix}\text{change in angular} \\ \text{momentum}\end{matrix},$$

where M_0 is the amplitude of the sinusoidal bending moment (N m), t is time (s), k is the angular stiffness (N m rad^{-1}), δ is the phase lag, or lag time, between the bending moment and the angular displacement (s), c is the damping coefficient (kg m^2 rad^{-2} s^{-1}) and I is the moment of inertia (kg m^2 rad^{-3}).

The equation of motion represents the bending moment as the sum of three forces – stiffness, damping and inertia. Thus, the mechanical behavior of the system is determined by the dynamic mechanical properties angular stiffness k, damping coefficient c, and moment of inertia I. Since the moment of inertia is a result of the mass of the intervertebral joint and not of the materials of the joint *per se*, in this study I focus on the elastic and viscous properties of the structure, angular stiffness and damping coefficient. These viscoelastic properties determine the transmission of moment through the intervertebral joint. As angular stiffness, k, increases, a greater bending moment, M_0, is needed to cause a given angular deformation, $\theta_0\sin\omega t$. Thus, for the same degree of bending, a stiffer joint resists a greater bending moment and, at the same time, transmits that bending moment to whatever it is attached (Newton's third law). Meanwhile, the damping coefficient, c, determines how much of the bending moment is proportional to the angular velocity, as is shown in the following equation (Denny, 1988):

$$c = \frac{\tan\delta(k - I\omega^2)}{\omega}. \quad (2)$$

When the phase lag, δ, is zero, c is zero and all of the moment used to bend the joint is in phase with the displacement and returned elastically as a function of k. As δ increases, up to one-quarter of the wavelength, the elastic moment that is returned decreases, c is greater than zero, and the system, which is now losing energy, is damped (Denny, 1988).

Materials and methods

Intervertebral joints

I tested nine of the 23 intervertebral joint positions of the blue marlin: precaudal joint positions 3, 5, 7 and 9, transitional joint position 11 (between the last precaudal and first caudal vertebrae) and caudal joint positions 13, 15, 17 and 19. The number of each intervertebral joint corresponds to the number of the vertebra anterior to it. Six joints of positions 3, 5, 7, 13, 17 and 19 and five joints of positions

9, 11 and 15 were taken from six fresh blue marlin collected from local fish houses in Kailua-Kona, Hawaii. The marlin were caught on hook and line and put into cold storage no longer than 8 h after capture.

The intact marlin weighed 29.3, 48.5, 79.2, 83.0, 93.4 and 96.6 kg (mean weight 71.7 kg) and were stored for 24–72 h at 4 °C. Since the heads were removed before I received the backbones, I used the overall weight of each marlin to estimate its length from the anterior tip of the lower jaw to the fork of the tail (E. C. Cyr, J. M. Dean, I. Jehangeer, M. Nallee, unpublished data). From lowest to highest weight, the estimated lengths were 1.40 m, 1.65 m, 1.90 m, 1.95 m, 2.00 m and 2.03 m (mean length 1.82 m). Backbones, once removed, were kept bathed in marine teleost saline (Pantin, 1964) and on ice until testing.

Intervertebral joints, left attached to adjacent vertebrae (as in Fig. 1), were tested individually. Each joint was warmed to room temperature (27–32 °C) before, and continually bathed in saline during, the mechanical tests.

Mechanical testing

For each intervertebral joint, angular frequency, ω, and bending amplitude, θ_0, were varied and bending moment, M_0, and phase lag, δ, were measured in response. The bending motion was sinusoidal and varied over a range of bending frequencies (0.5–5 Hz) that included the range of tailbeat frequencies for hooked and free-swimming marlin (approximately 1–2 Hz) seen on underwater video tapes taken by Stephen Wainwright at Duke University and Sharkbait Productions, Kona, Hawaii. The following discussion uses both bending frequency, f, in Hertz, and angular frequency, ω, in radians per second. Since the curvature of marlin during swimming could not be quantified from the videotapes, the range of bending amplitudes for each intervertebral joint was roughly estimated to be between 0 and 5.0°. For mechanical testing, two bending amplitudes, ±3.3° and ±5.0°, were used.

The bending machine in Fig. 2 converted the rotary motion of a motor into a reciprocating bending motion with an amplitude that varies as a sinusoidal function of time. In order to be tested, each intervertebral joint was positioned with its lateral bending axis, presumed to run through the middle of the joint, collinear with the axis of the shaft D, perpendicular to the page in Fig. 2.

Bending frequencies ranged in 0.5 Hz increments from 0.5 Hz to 5 Hz. Occasional zero-offset errors caused the maximum bending frequency for some tests to reach 7 Hz. The resonance frequency of the machine, with and without loaded intervertebral joints, was approximately 12 Hz. Bending frequency was controlled with a Minarik model SL-52 speed control attached to the motor and was measured directly using a Schaevitz Engineering model R30D rotary variable differential transducer (RVDT) (125 mV degree^{-1}, 0.25 % linearity) mounted coaxially with the rotating shaft (point D, Fig. 2). The displacement signal from the RVDT was digitally sampled at 500 points per second using a National Instruments model NB-MIO-16 16 bit analog-to-digital converter and LabVIEW software with an Apple MacIntosh IIcx. For any chosen bending frequency,

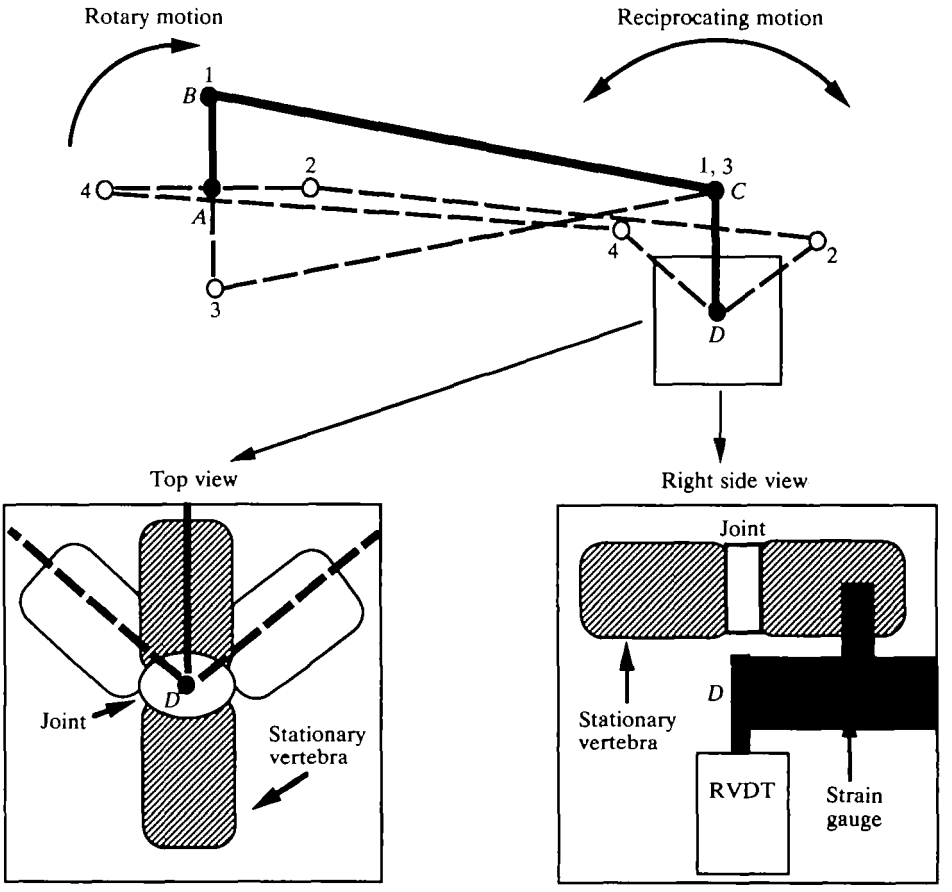

Fig. 2. Linkage diagram of bending machine. A motor turns shaft A, which is connected to shaft B by input linkage AB. All shafts (A, B, C and D) are perpendicular to the page, except shaft D in the right side view. As A rotates, B rotates through positions 1–4. The input linkage AB moves the connector linkage BC back and forth, causing the output linkage CD to oscillate in a reciprocating motion through positions 1–4. The top view shows a close up of the bending intervertebral joint at shaft D. The intervertebral joint is mounted directly above D, as seen in the right side view. One attached vertebra is held stationary, while the other vertebra is clamped to the output linkage, CD. The right side view shows the position of the rotary variable differential transducer (RVDT) coaxial with shaft D, and the placement of the strain gauge on output linkage CD.

fluctuations in motor speed and measurement imprecision combined for a repeatability, or imprecision, in angular frequency of ±2% (range) about the mean with a resolution, or inaccuracy, of $0.002\,\mathrm{rad\,s^{-1}}$.

Bending amplitude was controlled by changing the length of the input linkage (line $\overline{AB}$, Fig. 2). Resolution of the amplitude measurements was 0.006 rad.

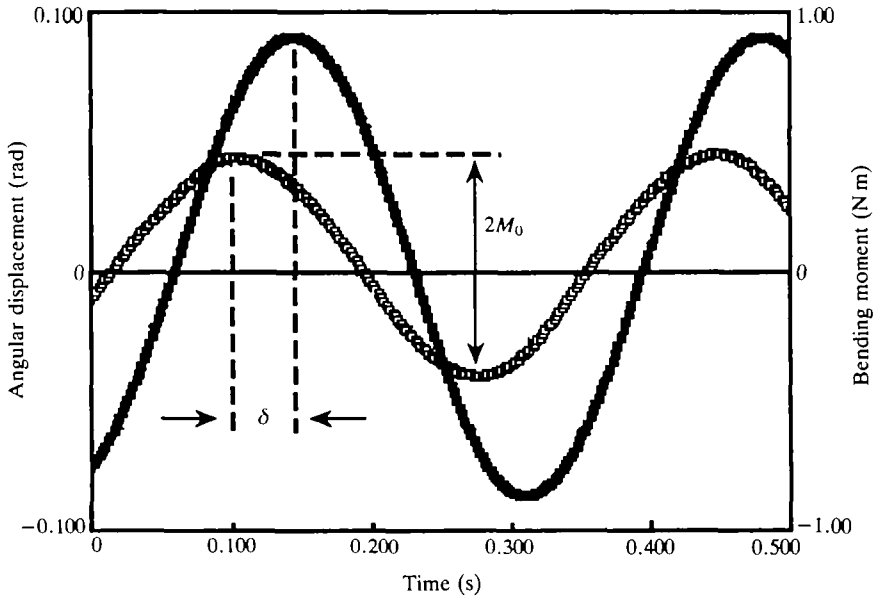

Fig. 3. Typical dynamic bending data. Filled squares indicate the sinusoidal angular (bending) displacement. Open squares indicate the sinusoidal bending moment causing the motion. δ is the phase lag between the angular displacement and the bending moment. $2M_0$ is twice the amplitude of the bending moment.

Dynamic measurements

The bending moment causing the sinusoidal motion (M_0, Fig. 3) was measured with two 120 Ω foil strain gauges mounted on the steel output linkage (line $\overline{CD}$, Fig. 2). The strain gauges were calibrated using calibrated weights. The moment arm of the output linkage was 11.7 cm and at that distance the gauges were sensitive to a deformation caused by a force of 0.1 N, which yields a moment resolution of approximately 0.01 N m. The strain gauge signal was generated using a bridge amplifier designed by Steven Vogel of Duke University with an Intersil commutating auto-zero instrumentation amplifier, model number CJN7605 (rated to 10 Hz). The bending moment signal was sampled at 500 points per second in the same manner as the angular deformation with a 3 % range of repeatability.

The other measured response to dynamic bending deformation was the phase lag (δ, Fig. 3), the time between the maximum angular displacement and the maximum bending moment. It was measured as the time between the zero-crossings of the moment and displacement signals and was converted to radians to normalize for each bending frequency. Resolution of phase lag was 0.002 s, with a 10 % range of repeatability.

Derived quantities

The moment of inertia, I, for each mounted joint and the moving parts of the machine was determined using the following method. First, by choosing a time, t,

so that the quantity $\omega t - \delta$ was equal to $\pi/2$ rad (90°), the damping (cosine) term became zero and equation 1 was simplified:

$$M_0 \sin(\omega t) = k\theta_0 - I\theta_0\omega^2 . \quad (3)$$

The only unknowns were k and I, so that choosing two bending frequencies, ω_1 and ω_2, with their associated values of M_0 and θ_0, produced two equations whence the two unknowns were determined. This method assumed that k and I were constant in both equations. This assumption was valid for I since only the frequency and not the mass of the system changes during the testing of each joint. This assumption, however, was problematic for k, since at this stage values of k were unknown. To minimize the error in measuring I, values from the two highest bending frequencies, when inertial moments are greatest, were used to calculate I. To measure the effect of assuming constant k, I was computed independently for each experiment using values from tests conducted at amplitudes of ±3.3° and ±5.0°. The resolution of I was 0.0001 kg m^2 rad^{-3} with a 5% range of repeatability.

At each angular frequency for a given bending amplitude, angular stiffness, k, was computed by substituting the calculated value for I back into equation 3. This yielded a resolution of 0.01 N m rad^{-1} and a 5% range of repeatability.

Damping coefficient, c, was computed independently of both k and I. When the damping force is maximal, velocity is maximal and the displacement is zero. Hence, c was calculated, with a resolution of 0.01 kg m^2 rad^{-2} s^{-1}, from the following equation:

$$M_0 \sin(\omega t) = c\omega\theta_0 . \quad (4)$$

Finally, the bending machine and the computational methods described above were calibrated using a polyurethane beam, provided by Jim Wilson of Duke University, with independently measured values of k and c. For k, the inaccuracy of the calibrated system averaged 5% over the frequency range of 0.5–5.0 Hz, with a 7% drop at 5.0 Hz. For c, the range of repeatability was 10%, with no frequency dependence.

Experimental protocol

Each intervertebral joint was tested using the following experimental protocol. After being clamped into the bending machine, each joint was preconditioned for approximately 30 s at a bending frequency of 2 Hz. Preconditioning stabilizes the mechanical behavior of the joint, a process that yields repeatable dynamic properties in articular cartilage (Woo *et al.* 1987) and a stable moment amplitude (Fig. 3) after several bending cycles at each new test frequency in the joint. After the initial preconditioning, the joint was bent at each of the 10 bending frequencies, starting with 0.5 Hz and increasing in 0.5 Hz increments to 5.0 Hz. This frequency sweep was made first at a bending amplitude of ±3.3° and then at a bending amplitude of ±5.0°. At each frequency, data were collected after at least 10 bending cycles.

For each frequency and amplitude, a computer file was created to store the simultaneous bending displacement and bending moment signals. I measured M_0, the amplitude of the bending moment curve, and δ, the time in seconds between maximum bending displacement and maximum bending moment (Fig. 3), using National Instrument's LabVIEW software. Each value of M_0 and δ for each frequency and amplitude was the average of five successive measurements along the time axis. For any joint, the mechanical behavior was stable over time – data taken at a specific frequency during the testing protocol did not differ significantly from data taken afterwards.

Statistical design

This statistical analysis was designed to test the hypothesis that the mechanical properties, k and c, change as a result of changes in bending frequency, bending amplitude and joint position. In addition, variation due to size differences between marlin was taken into account.

Since k and c were measured repeatedly at successively higher bending frequencies on the same joint, the measurements were dependent through time. Thus, I could not compare regressions of k or c onto bending frequency using analysis of covariance (Sokal and Rohlf, 1981). Instead, I compared the means of the regression parameters for each joint position and bending amplitude using t-tests (Sokal and Rohlf, 1981) and the Bonferroni procedure to account for multiple comparisons (Wilkinson, 1989). This method is analogous to a profile analysis of variance (Simms and Burdick, 1988).

To account for between-animal variation in size, I repeated the analysis with length-specific regression parameters. Within a given marlin, the regression parameters were normalized by the length of the vertebral column from vertebra 2 to vertebra 20. For marlin with body weights of 29.3, 48.5, 79.2, 83.0, 93.4 and 96.6 kg, these lengths, L, were, respectively, 88.0, 99.4, 116.7, 119.5, 122.8 and 108.6 cm.

The mechanical experiments at each joint position were replicated using six marlin. There were six replicates for joint positions 3, 5, 7, 13, 17 and 19 and five replicates for joint positions 9, 11 and 15.

Using r^2 values as the criterion, the best-fitting regression of angular stiffness, k, onto bending frequency was a linear regression. The same was true for damping coefficient, c. The regressions and all other statistics were calculated using the Systat Statistical Package, version 5.0 on the Apple MacIntosh IIcx (Wilkinson, 1989).

For angular stiffness, k, the intercept of the y-axis can be thought of as the stiffness of the intervertebral joint at rest, the so-called static angular stiffness. The slope of the line is the frequency response of stiffness, the change in k with the rate of deformation. The intercept of damping coefficient, c, has no simple mechanical interpretation. However, the slope of the line is the frequency response of the damping coefficient.

Morphometrics

I measured the following intervertebral and vertebral characters (Fig. 1): length of vertebral centra anterior and posterior to the joint, length of intervertebral ligaments (Fig. 1A); transverse height and width of the intervertebral capsule; and transverse lateral thickness of the intervertebral capsule (Fig. 1B). All morphometric measurements were made using Monostat model 6921 calipers with an accuracy of ±0.1 mm. Imprecision of the morphometrics ranges by ±6 % about the mean.

The lengths of the vertebral centra, anterior and posterior to the joint, were chosen because (1) each centrum can be thought of as a lever arm that bends the intervertebral joint and (2) each centrum has zygapophyses and neural and hemal spines that affect stiffness (Hebrank *et al.* 1990). The length of the intervertebral ligaments was chosen because it is a direct measure of the axial size of the joint, which should scale with stiffness. Transverse height, width and lateral thickness of the intervertebral capsule were chosen because similar dimensions are used to calculate the second moment of area, which determines flexural stiffness in man-made structures (Den Hartog, 1949).

To determine which subset of these morphological characters was the best predictor of k and c, I performed step-wise multiple regressions. The intercepts and slopes of the regression of angular stiffness, k, and damping coefficient, c, onto bending frequency were used as separate dependent variables and the morphological characters were the independent variables. Independent variables that were not normally distributed were log-transformed.

Results

Mechanical properties

The means and standard deviations of the intercepts and slopes of the regressions of angular stiffness, k, and damping coefficient, c, onto bending frequency, f, are given for each intervertebral joint at each bending amplitude in Table 1. The following significant differences were found ($\alpha<0.05$ using the Bonferroni procedure).

Amplitude effects on stiffness

The means of angular stiffness intercepts at bending amplitude ±3.3° are less than the means at amplitude ±5.0° for joint positions 11, 13, 17 and 19. The same trend holds for the length-specific intercepts with the addition of joint position 15.

Position effects on stiffness

At a bending amplitude of ±3.3°, the mean of the intercept of joint position 13 is greater than that of joint position 7. The mean of joint position 17 is greater than the means of joint positions 3, 7 and 13. For length-specific intercepts at this bending amplitude, the mean of joint position 13 is greater than the means of

Table 1. *Means and standard deviations of the intercepts and slopes of angular stiffness,* k, *and damping coefficient,* c

		Joint 3		Joint 5		Joint 7		Joint 9		Joint 11		Joint 13		Joint 15		Joint 17		Joint 19	
	Amplitude	±3.3°	±5.0°	±3.3°	±5.0°	±3.3°	±5.0°	±3.3°	±5.0°	±3.3°	±5.0°	±3.3°	±5.0°	±3.3°	±5.0°	±3.3°	±5.0°	±3.3°	±5.0°
Angular stiffness																			
Intercept	Mean	2.36	2.86	3.00	3.58	4.11	4.87	5.10	5.93	5.89	7.31	5.62	6.88	6.00	7.78	6.64	7.96	5.92	7.32
	S.D.	1.00	1.31	0.78	1.07	1.56	1.83	2.01	2.39	2.00	2.57	1.84	2.18	1.41	2.18	1.89	2.40	1.87	2.32
Slope	Mean	0.02	−0.06	0.03	−0.08	−0.03	−0.13*	−0.11	−0.20*	−0.13	−0.30*	0.00	−0.17*	−0.02	−0.30*	−0.12	−0.27*	−0.06	−0.27*
	S.D.	0.08	0.15	0.11	0.13	0.13	0.12	0.11	0.14	0.16	0.19	0.16	0.15	0.22	0.07	0.12	0.15	0.20	0.20
Damping coefficient																			
Intercept	Mean	0.056	0.058	0.060	0.059	0.058	0.061	0.076	0.075	0.071	0.082	0.077	0.098	0.073	0.085	0.111	0.105	0.080	0.092
	S.D.	0.017	0.015	0.020	0.020	0.024	0.034	0.024	0.018	0.022	0.035	0.031	0.034	0.036	0.026	0.036	0.037	0.022	0.030
Slope	Mean	−0.005*	−0.006*	−0.005*	−0.004*	−0.002	−0.001	−0.004	−0.001	0.000	0.002	−0.002	−0.005	0.002	0.002	−0.007	−0.003	−0.001	0.000
	S.D.	0.002	0.001	0.003	0.003	0.004	0.005	0.005	0.004	0.006	0.008	0.008	0.006	0.008	0.009	0.008	0.008	0.006	0.002

For bending amplitudes of ±3.3° and ±5.0°, each mechanical property was linearly regressed onto bending frequency (Hz).
Means of slopes different from a slope of zero, as determined using a *t*-test, are indicated by an asterisk ($P<0.05$).

positions 3 and 7, the mean of joint position 15 is greater than the means of positions 3 and 5, the mean of joint position 17 is greater than the means of positions 3, 5, 7 and 13, and the mean of joint position 19 is greater than the means of positions 3 and 5.

Position effects on stiffness

At a bending amplitude of ±5.0°, the mean of the intercept of joint position 13 is significantly greater than the mean of joint position 3. At the same amplitude, the mean of the intercept of joint position 17 is greater than that of joint positions 3 and 7. For length-specific intercepts at this amplitude, the mean of joint position 13 is greater than the mean of position 3, the mean of joint position 17 is greater than the means of positions 3, 5 and 7, and the mean of joint position 19 is greater than the mean of joint position 3.

Amplitude effects on frequency-dependence of stiffness

The mean of angular stiffness slopes at a bending amplitude of ±3.3° is significantly greater than the mean of angular stiffness slopes at an amplitude of ±5.0° for joint positions 13 and 19. The means of the length-specific slopes follow the same pattern.

Frequency effects on stiffness

The means of the slopes of joint positions 7–19 at a bending amplitude of ±5.0° are significantly less than zero.

Position effects on damping coefficient

At a bending amplitude of ±5.0°, the mean of the damping coefficient intercept of joint position 19 is significantly greater than the mean of the intercept of joint position 7. For length-specific intercepts, there are no significant differences.

Position effects on frequency-dependence of damping coefficient

At a bending amplitude of ±5.0°, the mean of the damping coefficient slope of joint position 19 is significantly greater than the mean of the slope of joint position 3. For length-specific damping slope, the mean of joint position 19 is greater than the mean of joint position 3 at both bending amplitudes.

Frequency effects on damping coefficient

At both bending amplitudes, the means of the slopes of the damping coefficients for joint positions 3 and 5 are significantly less than zero.

Angular stiffness and damping coefficient as a function of bending frequency are shown by bending amplitude and joint position in Figs 4, 5 and 6.

Functional vertebral morphology

The morphometrics of the intervertebral joints and associated vertebrae are

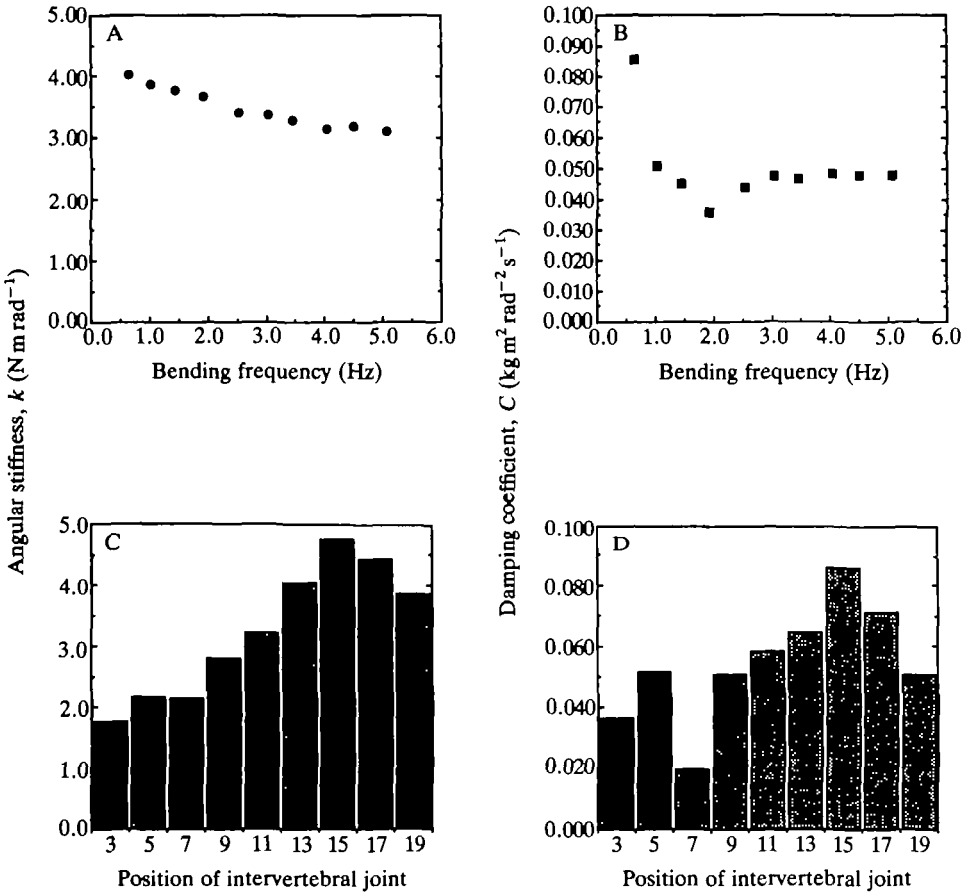

Fig. 4. Typical dynamic bending properties from a 29.3 kg blue marlin. These results are from joints bent at an amplitude of ±5.0°. (A) Angular stiffness as a function of bending frequency for joint 19. (B) Damping coefficient as a function of bending frequency for joint 19. (C) Angular stiffness for all the joint positions of this marlin at a bending frequency of 1 Hz. (D) Damping coefficient for all the joint positions of this marlin at a bending frequency of 1 Hz.

given in Table 2. The lengths of the centra anterior and posterior to the intervertebral joints increase until joint 15–17, and then decrease in length towards the tail. The transverse lateral thickness of the intervertebral joint is the only other measurement to show a similar pattern. The transverse height of the joint decreases from head to tail. The axial joint length and the transverse width of the joint vary only slightly.

The morphological characters that best predict the intercepts and slopes of the regression of angular stiffness and damping coefficient onto bending frequency are given in Table 3. At both bending amplitudes, 88 % of the variation in the intercept of angular stiffness is explained by the variation in three morphological

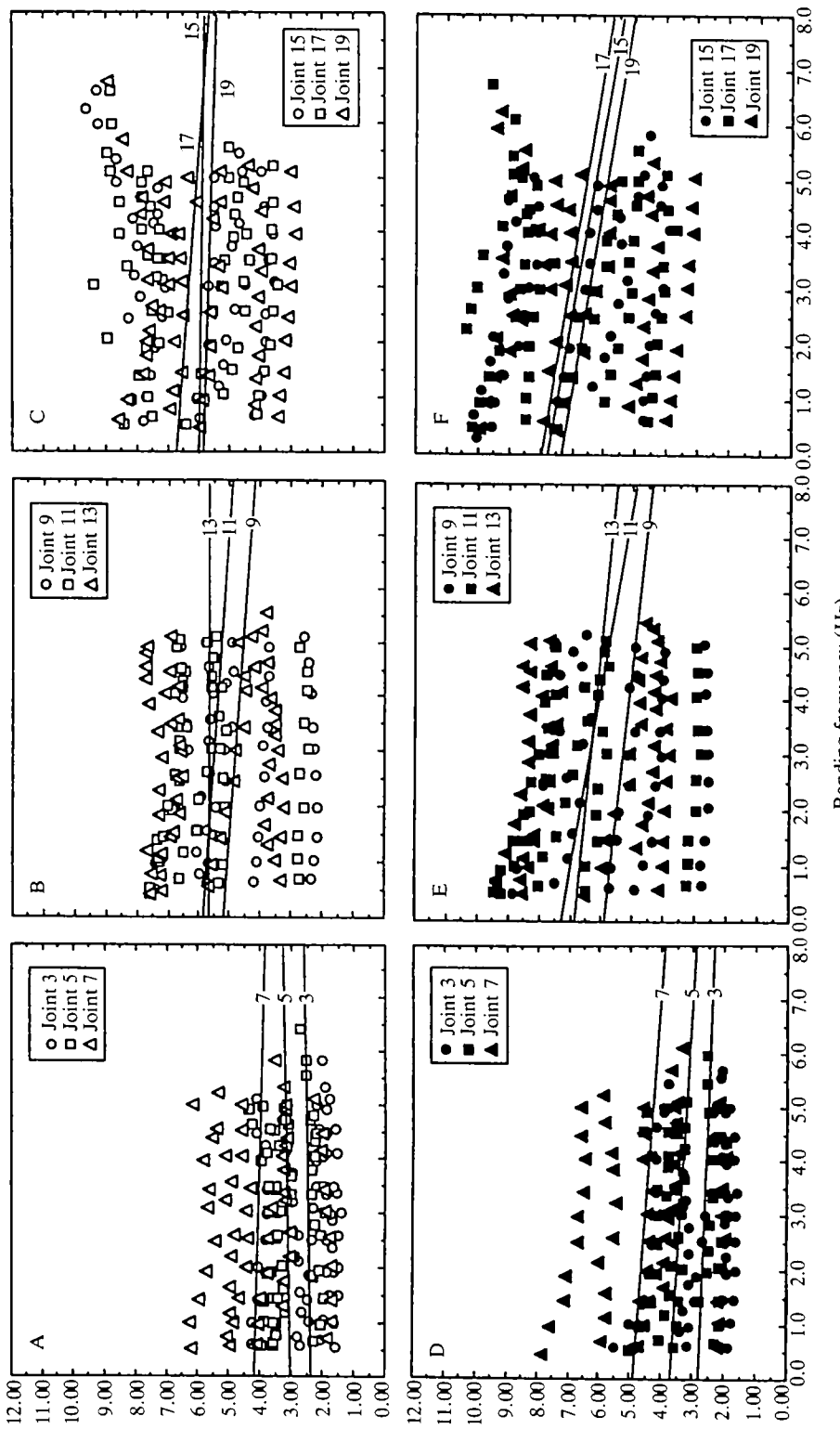

Fig. 5. Angular stiffness as a function of bending frequency. The average response at each joint position is drawn as a separate line. Lines are generated from mean regression coefficients given in Table 1. Numbers associated with lines indicate joint position. (A) Joint positions 3, 5 and 7 at a bending amplitude of ±3.3°. (B) Joint positions 9, 11 and 13 at a bending amplitude of ±3.3°. (C) Joint positions 15, 17 and 19 at a bending amplitude of ±3.3°. (D) Joint positions 3, 5 and 7 at a bending amplitude of ±5.0°. (E) Joint positions 9, 11 and 13 at a bending amplitude of ±5.0°. (F) Joint positions 15, 17 and 19 at a bending amplitude of ±5.0°. Statistically significant differences between regression lines are stated in the Results section.

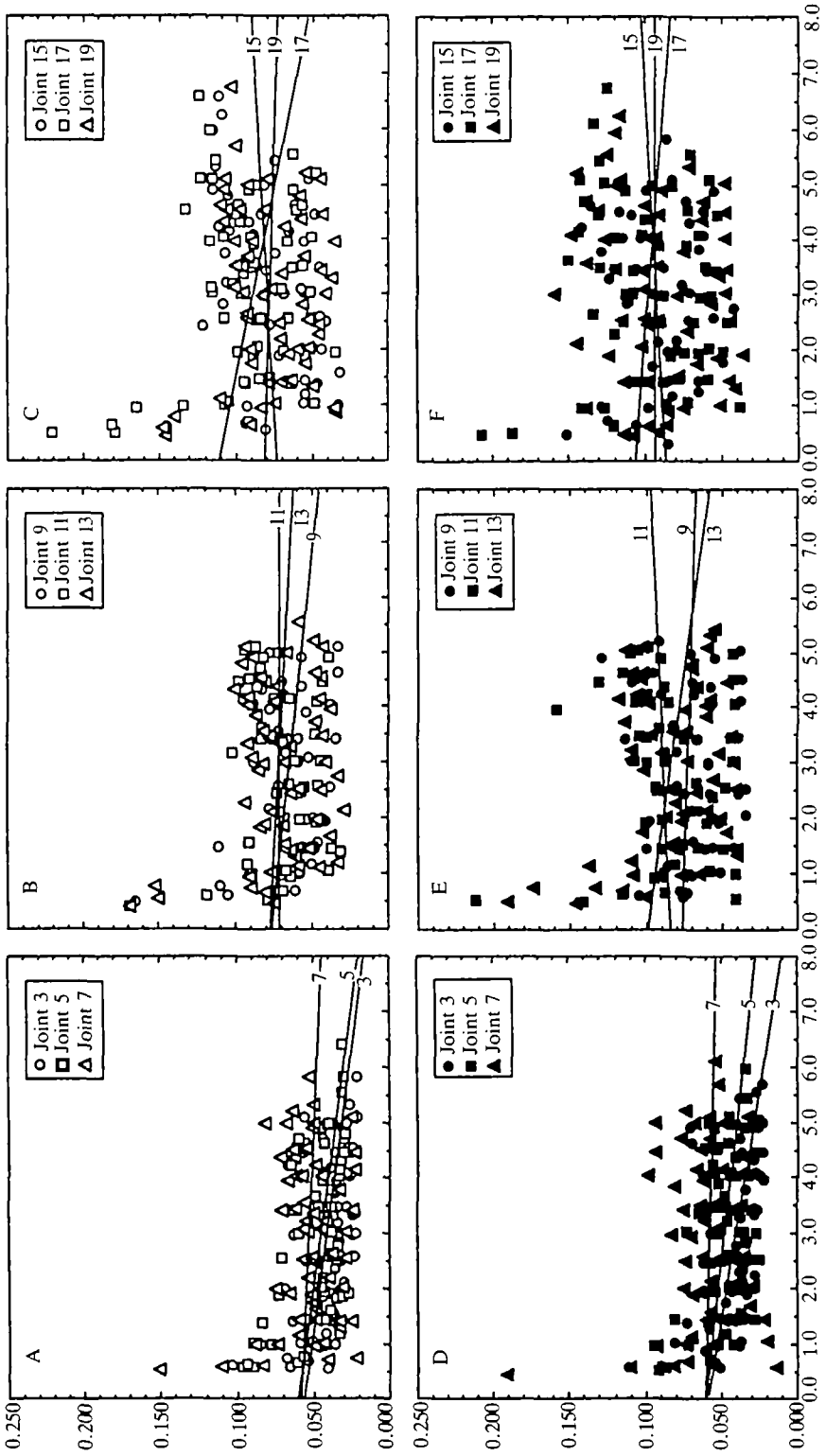

Fig. 6. Damping coefficient as a function of bending frequency. Data points for all joint positions and amplitudes are drawn. The lines represent the average regression line for each joint position (Table 1). Numbers associated with lines indicate joint position. (A) Joint positions 3, 5 and 7 at a bending amplitude of ±3.3°. (B) Joint positions 9, 11 and 13 at a bending amplitude of ±3.3°. (C) Joint positions 15, 17 and 19 at a bending amplitude of ±3.3°. (D) Joint positions 3, 5 and 7 at a bending amplitude of ±5.0°. (E) Joint positions 9, 11 and 13 at a bending amplitude of ±5.0°. (F) Joint positions 15, 17 and 19 at a bending amplitude of ±5.0°. Statistically significant differences between regression lines are stated in the Results section.

Table 2. *Means and standard deviations (in parentheses) of the morphological characters for each joint*

Joint	Axial joint length	Transverse joint height	Transverse joint width	Transverse lateral thickness	Anterior centrum length	Posterior centrum length
3 (N=6)	0.8 (0.2)	2.9 (0.4)	3.2 (0.5)	0.9 (0.2)	3.6 (0.5)	3.9 (0.5)
5 (N=6)	0.8 (0.2)	2.6 (0.3)	3.0 (0.4)	0.9 (0.2)	4.1 (0.5)	4.6 (0.7)
7 (N=6)	0.8 (0.1)	2.5 (0.4)	3.0 (0.5)	1.1 (0.3)	5.1 (0.6)	5.6 (0.8)
9 (N=5)	0.8 (0.2)	2.5 (0.4)	3.1 (0.5)	1.2 (0.3)	6.2 (0.9)	6.3 (0.8)
11 (N=5)	0.8 (0.2)	2.4 (0.4)	3.3 (0.5)	1.5 (0.2)	6.6 (0.9)	6.8 (0.9)
13 (N=6)	0.8 (0.2)	2.1 (0.3)	3.2 (0.5)	1.5 (0.3)	5.7 (2.9)	7.1 (0.8)
15 (N=5)	0.9 (0.6)	1.9 (0.4)	3.2 (0.6)	1.7 (0.4)	7.2 (0.9)	7.3 (0.9)
17 (N=6)	0.8 (0.2)	1.9 (0.3)	3.1 (0.5)	1.6 (0.2)	7.5 (0.9)	7.2 (0.8)
19 (N=6)	0.9 (0.3)	1.9 (0.2)	2.8 (0.5)	1.5 (0.4)	7.1 (0.9)	6.4 (1.0)

The number of samples of each joint position are given.
Measurements are in centimeters.

characters. For the slope of angular stiffness, only 13 % and 36 % of the variation, for amplitudes of ±3.3° and ±5.0°, respectively, is explained by the variation in two morphological characters. For damping coefficient, only the intercept at a bending amplitude of ±5.0° has more than 50 % of its variation explained by variation in the morphological characters.

Examination of the standardized coefficients, which account for the differences in size between the morphological characters, shows that, for angular stiffness, the most important variable is the logarithm of the length of the anterior centrum. For the intercept of damping coefficient, length of the posterior centrum is most important. For the slope of the damping coefficient, the most important variables are width of the intervertebral capsule at ±3.3° and transverse thickness of the intervertebral ligaments at ±5.0°.

Discussion

The equation of motion, which describes the relationship between force and motion, has been used to determine the mechanical properties that are important to the dynamic functions of intervertebral joints. This approach has yielded several insights. First, the mechanical properties of angular stiffness and damping coefficient vary with the motion of the joint. Second, there is regional variation in angular stiffness and in damping coefficient; this variation is correlated with structural variation. Third, the mechanics of the intervertebral joints are dominated by stiffness moments.

Bending motion changes the mechanical properties of intervertebral joints

The angular stiffness of the intervertebral joints is a variable mechanical

Table 3. *Predictor equations for the regression coefficients of angular stiffness and damping coefficient*

	Amplitude	Variable	Coefficient	Standardized coefficient	*P* value	Overall r^2	Overall *P*
Angular stiffness							
Intercept	±3.3°	Constant	−9.995	0.000	0.000		
		Width	1.433	0.329	0.000		
		log ant. cent.	15.297	0.914	0.000		
		Thickness	−0.909	−0.172	0.092		
						0.881	0.000
	±5°	Constant	−12.588	0.000	0.000		
		Width	1.873	0.341	0.000		
		log ant. cent.	16.533	0.783	0.000		
		log length	−2.020	−0.092	0.118		
						0.879	0.000
Slope	±3.3°	Constant	0.323	0.000	0.029		
		log ant. cent.	−0.738	−0.614	0.018		
		Thickness	0.150	0.395	0.120		
						0.127	0.041
	±5.0°	Constant	0.422	0.000	0.001		
		log ant. cent.	−0.810	−0.604	0.000		
						0.365	0.000
Damping coefficient							
Intercept	±3.3°	Constant	0.007	0.000	0.670		
		Post. cent.	0.011	0.516	0.000		
						0.266	0.000
	±5.0°	Constant	−0.060	0.000	0.027		
		Post. cent.	0.017	0.760	0.000		
		log length	−0.065	−0.242	0.028		
		Height	0.012	0.180	0.097		
						0.516	0.000
Slope	±3.3°	Constant	−0.012	0.000	0.027		
		Height	−0.004	−0.304	0.086		
		Width	0.006	0.472	0.009		
						0.134	0.031
	±5.0°	Constant	−0.006	0.000	0.034		
		Thickness	0.004	0.298	0.032		
		log length	0.012	0.257	0.063		
						0.200	0.005

Morphological predictors were chosen using stepwise linear regression of all morphological variables.

Note that length of intervertebral joint (length) and length of anterior centrum (ant. cent.) are log-transformed.

See Table 2 for a complete list of morphological variables.

property, changing as a function of bending amplitude and frequency (Figs 4 and 5). In a swimming fish, bending amplitude increases along the body and tailbeat (bending) frequency changes with swimming speed (Videler and Hess, 1984; Webb, 1986). What effect might these changes in swimming motion have on the mechanics and functions of the intervertebral joints? With increasing bending amplitude, increases in angular stiffness of the intervertebral joints would, for each increment of angular displacement, cause the intervertebral joints to transmit proportionally more bending moment. This non-linear increase in stiffness with strain is called 'spring hardening' (Timoshenko *et al.* 1974) and is typical of statically deformed teleost intervertebral joints (Hebrank, 1982; Hebrank *et al.* 1990) and other connective tissues (Wainwright *et al.* 1976). In contrast, with increases in tailbeat frequency, the transmitted moment would actually decrease slightly, since the rate of increase with bending frequency of many of the intervertebral joint positions is negative.

This negative response of angular stiffness to increases in bending frequency must be viewed with some caution, since other viscoelastic polymers do not exhibit this behavior (Ferry, 1961). There are two classes of explanation for this phenomenon: (1) the intervertebral joints are built of novel materials or structures, or (2) the negative slope, seen only at bending amplitudes of $\pm 5.0°$, is a result of the 7 % drop in sensitivity of the bending machine at high frequencies (see Materials and methods). I favor the former explanation, since the smallest significant decrease from 0.5 to 5.0 Hz for a joint position is 13 %, while the largest is 21 %.

In addition to increasing the transmitted moment, amplitude-dependent increases in the angular stiffness of the intervertebral joints may increase the speed of the undulatory waves propagated down the vertebral column. This hypothesis is based on the fact that the speed at which a mechanical vibration is propagated through a homogeneous solid is proportional to the square root of the material's elastic modulus (Timoshenko *et al.* 1974). The elastic modulus is the proportionality constant of stress and strain, making it mechanically analogous to angular stiffness, k, which is the proportionality constant of bending moment and angular displacement (see equation 1).

In contrast to angular stiffness, damping coefficient, c, of the intervertebral joints is independent of the bending amplitude. However, damping coefficient does decrease with bending frequency at joint positions 3 and 5 (Table 1; Fig. 6). This frequency-dependent decrease in c is similar to the behavior of the mechanically analogous dynamic viscosity, η', as measured in amorphous viscoelastic polymers (Ferry, 1961). This drop in damping coefficient with increased bending frequency has two effects. First, the tangent of δ (see equation 2), which is an indicator of the proportion of energy dissipated (Wainwright *et al.* 1976), will not increase as quickly with frequency as it would if c were frequency-independent. Nonetheless, the behavior of $\tan\delta$ would be similar to that of viscoelastic polymers (Ferry, 1961; Wainwright *et al.* 1976). Second, since damping forces are proportional to the angular velocity, less damping force will be

generated by the joint with increased frequency than would be generated if c were frequency-independent.

Angular stiffness and damping coefficient vary regionally

Angular stiffness, k, as represented by the intercept of its regression onto bending frequency, is greater in the caudal intervertebral joint positions (13–19) than in the precaudal joint positions (3–7). This anterior–posterior difference is particularly clear when the regression intercepts are normalized for differences in size between the marlin tested. In contrast, the intercept of damping coefficient differs only between joint positions 7 and 19, a distinction that disappears when the intercepts are normalized for size. As suggested above, angular stiffness may function in the regulation of the speed at which an undulatory wave propagates through an intervertebral joint. Considering the vertebral column as a whole, the increase of angular stiffness along the vertebral column may accelerate the undulatory wave as it travels along the body. It has been suggested that an axial gradient of mechanical properties is a necessary condition of aquatic undulatory locomotion (Blight, 1977). For example, Webb (1973) described a reversible stiffness gradient in the notochord of *Branchiostoma* that is correlated with the alternating backward and forward propagation of undulatory waves. In the context of this study, however, it should be remembered that, although the flexibility of the body is affected by the stiffness of the vertebral column, muscle and skin play an important role as well.

A flexible anterior vertebral column may also function in feeding. Underwater videotapes, taken by Sharkbait Productions (Kona, Hawaii) of a free-swimming blue marlin approaching a live bait, show the marlin swinging its head in an attempt to strike the bait with its bill. Other footage shows a hooked blue marlin whipping its head from side to side in an attempt to dislodge the hook. These observations suggest that the marlin uses its relatively flexible 'neck' to bludgeon prey with its bill or dislodge over-size prey.

The regional variations in angular stiffness and damping coefficient are correlated with the variation in a number of the vertebral characters (Fig. 1; Tables 2 and 3). The variation in angular stiffness is the most tightly correlated with vertebral characters, the most important of which, according to the standardized regression coefficients, is the logarithm of the length of the centrum anterior to the intervertebral joint. At the same time, the length of the centrum posterior to the joint is the most important correlate of the intercept of the regression of damping coefficient onto bending frequency.

Why is the length of the vertebral centra correlated with angular stiffness and damping coefficient? Since the bony centrum is not part of the joint, there must be unmeasured structures correlated with centrum length, or size in general, that are mechanical determinants of k and c. Likely candidates are the interlocking zygapophyses and neural and hemal spines (Fig. 1), all of which span the intervertebral joint and vary in size along the vertebral axis. The zygapophyses have a measurable effect on lateral stiffness, since removing them partially reduces

quasi-static bending stiffness (Hebrank *et al.* 1990). It is interesting to note that such robust, interlocking processes are missing from the marlin's sister taxa, the swordfish *Xiphius gladius* (Gregory and Conrad, 1937) and the tunas and mackerels (Fierstine and Walters, 1968). Based on this inter-familial variation, I would predict correlated differences in the angular stiffness and damping coefficient in these related taxa.

The mechanics of the intervertebral joints are dominated by the effects of stiffness moments

For all intervertebral joint positions and bending frequencies, the maximal stiffness moments during bending are always greater, within a frequency range of 0.5–5.0 Hz, than the maximal damping moments (Fig. 7). Values of the moments for *in vivo* strain rates (1–2 Hz) are intermediate with respect to the extreme frequencies shown. The maximal stiffness moment, M_k, for each joint position was computed as the product of the angular stiffness for that frequency (from Table 1) and angular displacement, when t is chosen so that angular displacement is maximal:

$$M_k = k\theta_0(\sin\omega t)\,. \tag{5}$$

The maximal damping moment, M_c, for each joint position was computed as the

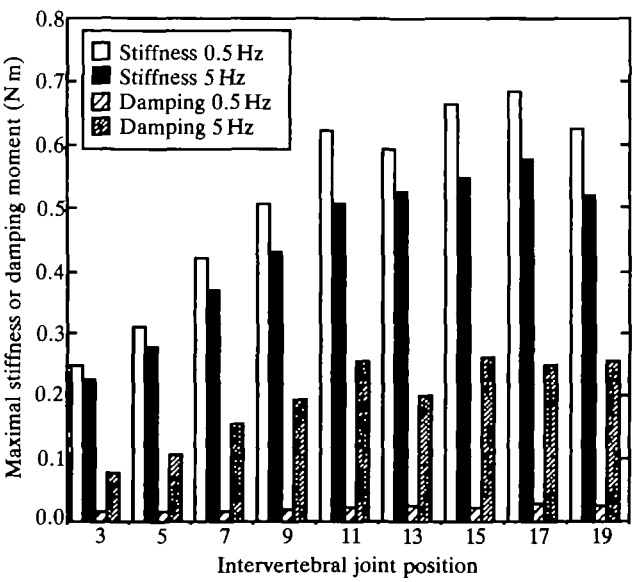

Fig. 7. Maximal stiffness and damping moments generated by the intervertebral joints during bending at ±5.0°. For each joint position, the mean maximal stiffness and damping moments from the six marlin are plotted at bending frequencies of 0.5 and 5.0 Hz. Only at 5.0 Hz do damping moments make up a sizable portion of the total maximal moment of each joint position. Stiffness moments are in phase with bending and damping moments are 90° out of phase with bending, leaving them in phase with angular velocity.

product of the damping coefficient (from Table 1) and the angular velocity, when t is chosen so that angular velocity is maximal:

$$M_c = c\omega\theta_0(\cos\omega t)\,. \tag{6}$$

Equations 5 and 6 show that the maxima of the two moments are 90° out of phase. Specifically, M_k is in phase with angular displacement, $\sin\omega t$, and M_c is in phase with angular velocity, $\cos\omega t$, which is the first derivative of displacement. This phase difference has several mechanical consequences for a sinusoidally bending intervertebral joint: (1) the maximal moment transmitted by the joint occurs when the joint is fully bent, (2) the overall maximal moment is not the sum of the stiffness and damping maxima, (3) a bending moment is transmitted by the damping moment when the joint is straight (velocity is maximal), and (4) as bending frequency increases, the maximal damping moment increases proportionally while the maximal stiffness moment remains relatively constant.

In addition to transmitting moments through the joint, the stiffness and damping moments cause the external moment creating the motion – be it of muscular or hydrodynamic origin – to do mechanical work. For a complete bending cycle, the work done by the external moment as a result of the stiffness and damping moments can be measured as the area under a power–time curve (Fig. 8). Power is calculated as the product of a force and a velocity, or, as in this angular case, the product of a moment and an angular velocity. The external power needed to overcome the stiffness moment at any time, t, is:

$$P_k = (k\theta_0\sin\omega t)(\omega\theta_0\cos\omega t)\,, \tag{7}$$

where the first term on the right-hand side of the equation is the stiffness moment (equation 5) and the second term is the angular velocity. The external power needed to overcome the damping moment at any time, t, is:

$$P_c = (c\omega\theta_0\cos\omega t)(\omega\theta_0\cos\omega t)\,, \tag{8}$$

where the first term on the right-hand side is the damping moment (equation 6). The total power needed to move the joint at any time t is the sum of equations 7 and 8. When the area under the power–time curve is positive, then the external moment has done positive work to bend the joint. Negative work means that the joint is doing work, i.e. the joint is returning elastically stored strain energy (Alexander, 1988). The net work over the complete cycle is the energy dissipated by the joint. Even at high bending frequencies, the energy dissipated is very small, of the order of 5–10%. In terms of energy return, this means that the intervertebral joints have a resilience of greater than 90%. This value is much higher than the 50–80% resilience reported by Hebrank *et al.* (1990) for caudal and precaudal sections of marlin vertebral columns bent quasi-statically. This discrepancy may be caused by two factors. First, low resiliences could be the result of a rate of strain faster than the 5 Hz measured in this study. However, the strain rates were not reported by Hebrank *et al.* (1990). Second, they bent the vertebral

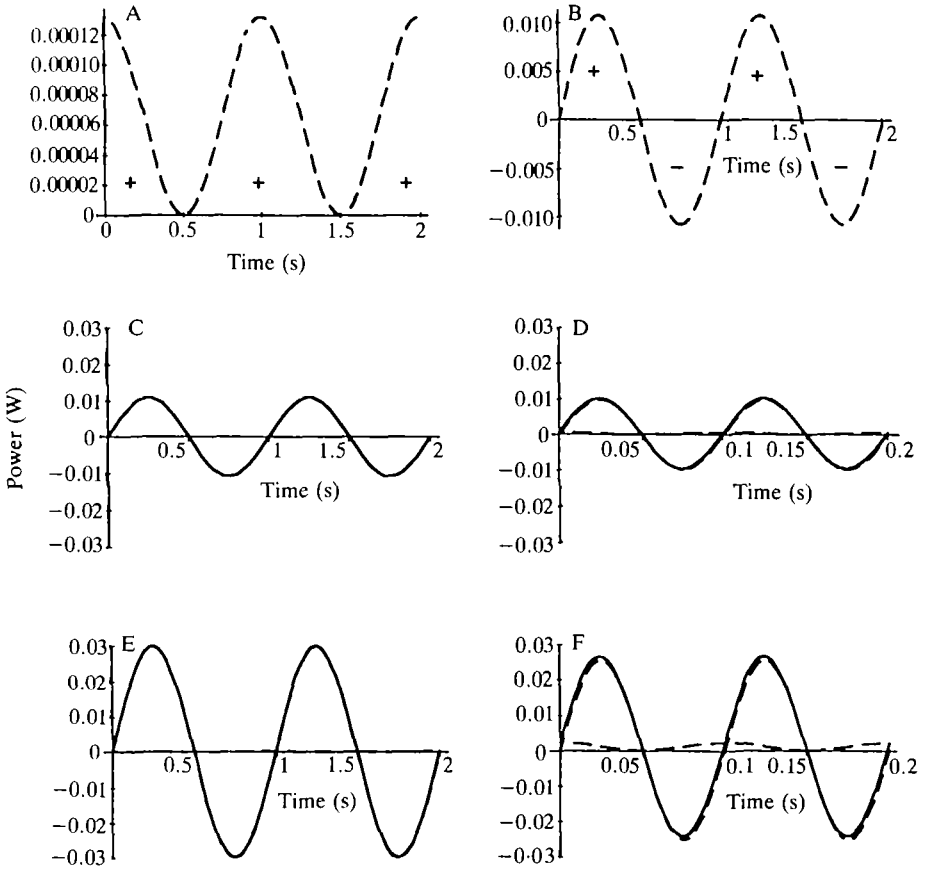

Fig. 8. Power curves for intervertebral joints bent at an amplitude of ±5.0°. The area under each power curve is the work done by the externally applied moment on the intervertebral joint. Dashed curves are the constituent stiffness and damping components of the total power curve (unbroken curves). (A) A full cycle of the damping power for joint position 3 at a bending frequency of 0.5 Hz. The work done by the external force is always positive, meaning that energy is always being expended to overcome the damping forces of the joint. (B) A full cycle of the stiffness power for joint position 3 at a bending frequency of 0.5 Hz. The work done by the external force alternates between positive and negative, meaning that the energy expended to overcome stiffness forces is returned in elastic recoil as negative work. (C) The sum of the damping and stiffness power for joint position 3 at a bending frequency of 0.5 Hz. (D) Power curves for joint position 3 at a bending frequency of 5.0 Hz. (E) Power curves for joint position 17 at a bending frequency of 0.5 Hz. (F) Power curves for joint position 17 at a bending frequency of 5.0 Hz.

column sections into C-shapes, incurring high bending strains well beyond those measured in this study.

Because the intervertebral joints are dominated by stiffness moments, the work-related functions of the joint are to provide (1) an elastic energy storage

mechanism during the negative work phase when the joint moves from a bent to an unbent position and (2) a muscle antagonist during the positive work phase when the joint moves from an unbent to a bent position. While there are many examples of the usefulness of energy return (Alexander, 1988), what are the functional consequences of energy loss in the intervertebral joints? One possible function of energy dissipation by the intervertebral joints may be dynamic stability. Meyhöfer and Daniel (1990) have argued that energy dissipation in muscle cells prevents high and potentially destructive internal strains in the tails of shrimp during escape locomotion. I suggest that the intervertebral joints, which develop substantial damping moments only at high tailbeat frequencies when locomotor power is maximal, may perform a similar function at high speeds in the blue marlin.

While moments external and internal to the intervertebral joints are the foci of this discussion, it is important to realize that, with one theoretical exception (Hess and Videler, 1984), the bending moments generated by muscles during locomotion remain enigmatic. In practice, muscular moments are difficult to measure because it is unclear what moment arms are used by the muscles. As this study demonstrates, sizable muscular moments could be transmitted by the vertebral column to the tail. In spite of increasingly sophisticated knowledge of the force, power and shortening velocities of muscle in swimming fish (e.g. Rome and Sosnicki, 1990; Rome *et al.* 1990), we still do not understand how the mechanical interactions of the muscle and vertebral column cause the fish to bend (Wainwright, 1983; Long *et al.* 1990).

List of symbols

c damping coefficient (in $kg\,m^2\,rad^{-2}\,s^{-1}$)
f bending frequency (in Hz)
I moment of inertia (in $kg\,m^2\,rad^{-3}$)
k angular stiffness (in $N\,m\,rad^{-1}$)
L length of vertebral column from vertebra 2 to vertebra 20 (in m)
L_A length of the vertebral centrum anterior to the joint (in cm)
L_J length of the intervertebral ligaments (in cm)
L_P length of the vertebral centrum posterior to the joint (in cm)
M_c maximal damping moment during a bending cycle (in N m)
M_k maximal stiffness moment during a bending cycle (in N m)
M_0 amplitude of bending moment (in N m)
P_c power of external moment needed to overcome damping moments (in W)
P_k power of external moment needed to overcome stiffness moments (in W)
t time (in s)
T_H transverse height of the intervertebral capsule (in cm)
T_W transverse width of the intervertebral capsule (in cm)
T_T transverse lateral thickness of the intervertebral capsule (in cm)
δ phase lag between bending displacement and bending moment (in s or rad)
θ_0 amplitude of bending displacement (in rad)
ω angular frequency (in $rad\,s^{-1}$)

I am indebted to Stephen A. Wainwright for challenging and inspiring discussions about backbones, gentle assistance in the field and laboratory, and constructive readings of the manuscript. I thank Steve Vogel for advice and guidance building the prototype of the dynamic bending machine. I thank John Hebrank for advice on refining later versions of the bending machine. I am grateful to Barbara Block for convincing me that marlin were worthy of study. For statistical advice, I thank Don Burdick and Mark Westneat. The field work in Hawaii was made possible by David Grobecker, Director of Pacific Ocean Research Foundation, and a grant from the Lerner–Gray Fund of the American Museum of Natural History. Manuscript readers who were of great help in early drafts and take no blame for the problems of the final version are Hugh Crenshaw, Mary and Jack Hebrank, Anne Moore, Margaret Ronsheim, V. Louise Roth, Kathleen Smith and Mark Westneat. Later versions were helped by two anonymous reviewers. Illustrations are by Rosemary Calvert. I was supported by a Morphology Fellowship from the Cocos Foundation of Indianapolis, Indiana.

References

ALEXANDER, R. MCN. (1988). *Elastic Mechanisms in Animal Movement.* Cambridge: Cambridge University Press.

BLIGHT, A. R. (1977). The muscular control of vertebrate swimming movements. *Biol. Rev.* **52**, 181–218.

CUVIER, G. AND VALENCIENNES, A. (1831). *Histoire Naturalle des Poissions*, vol. 8, Paris. (Reprinted by A. Asher, Amsterdam, 1969).

DEN HARTOG, J. P. (1949). *Strength of Materials.* New York: McGraw-Hill Book Company.

DEN HARTOG, J. P. (1956). *Mechanical Vibrations.* 4th edn. New York: McGraw-Hill Book Company.

DENNY, M. W. (1988). *Biology and the Mechanics of the Wave-Swept Environment.* Princeton, New Jersey: Princeton University Press.

FERRY, J. D. (1961). *Viscoelastic Properties of Polymers.* New York: John Wiley and Sons.

FIERSTINE, H. L. AND WALTERS, V. (1968). Studies in locomotion and anatomy of scombroid fishes. *Mem. south. Calif. Acad. Sci.* **6**, 1–67.

GREGORY, W. K. AND CONRAD, G. M. (1937). The comparative osteology of the swordfish (*Xiphias*) and the sailfish (*Istiophorus*). *Am. Mus. Novitates* **952**, 7–25.

HEBRANK, J. H., HEBRANK, M. R., LONG, J. H., JR, BLOCK, B. A. AND WAINWRIGHT, S. A. (1990). Backbone mechanics of the blue marlin *Makaira nigricans* (Pisces, Istiophoridae). *J. exp. Biol.* **148**, 449–459.

HEBRANK, M. R. (1982). Mechanical properties of fish backbones in lateral bending and in tension. *J. Biomechanics* **15**(2), 85–89.

HESS, F. AND VIDELER, J. J. (1984). Fast continuous swimming of saithe (*Pollachius virens*): a dynamic analysis of bending moments and muscle power. *J. exp. Biol.* **109**, 229–251.

HOME, E. (1809). On the nature of the intervertebral substance in fish and quadrupeds. *Proc. R. Soc. Lond.* **16**, 177–187.

JOHNSRUDE, C. I. AND WEBB, P. W. (1985). Mechanical properties of the myotomal musculoskeletal system of rainbow trout, *Salmo gairdneri*. *J. exp. Biol.* **119**, 171–177.

LONG, J. H., JR, WESTNEAT, M. W. AND WAINWRIGHT, S. A. (1990). The mechanics of undulation in the blue marlin *Makaira nigricans*. *Am. Zool.* **30**(4), 75A.

MEYHÖFER, E. AND DANIEL, T. (1990). Dynamic mechanical properties of extensor muscle cells of the shrimp *Pandalus danae*: cell design for escape locomotion. *J. exp. Biol.* **151**, 435–452.

PANTIN, C. F. A. (1964). *Notes on Microscopical Technique for Zoologists.* Cambridge: Cambridge University Press.

ROCKWELL, H., EVANS, F. G. AND PHEASANT, H. C. (1938). The comparative morphology of the vertebrate spinal column: its form as related to function. *J. Morph.* **63**, 87–117.

ROME, L. C., FUNKE, R. P. AND ALEXANDER, R. M. (1990). The influence of temperature on muscle velocity and sustained performance in swimming carp. *J. exp. Biol.* **154**, 163–178.

ROME, L. C. AND SOSNICKI, A. A. (1990). Influence of temperature on mechanics of red muscle in carp. *J. Physiol., Lond.* **427**, 151–169.

SIMMS, E. L. AND BURDICK, D. S. (1988). Profile analysis of variance as a tool for analyzing correlated responses in experimental ecology. *Biometr. J.* **2**, 229–242.

SOKAL, R. R. AND ROHLF, F. J. (1981). *Biometry*. 2nd edn. New York: W. H. Freeman and Company.

SYMMONS, S. (1979). Notochordal and elastic components of the axial skeleton of fishes and their functions in locomotion. *J. Zool., Lond.* **189**, 157–206.

TIMOSHENKO, S., YOUNG, D. H. AND WEAVER, W., JR (1974). *Vibration Problems in Engineering*. 4th edn. New York: John Wiley and Sons.

VAN LEEUWEN, J. L., LANKHEET, M. J. M., AKSTER, H. A. AND OSSE, J. W. M. (1990). Function of red axial muscles of carp (*Cyprinus carpio*): recruitment and normalized power output during swimming in different modes. *J. Zool., Lond.* **220**, 123–145.

VIDELER, J. J. AND HESS, F. (1984). Fast continuous swimming of two pelagic predators, saithe (*Pollachius virens*) and mackerel (*Scomber scombrus*): a kinematic analysis. *J. exp. Biol.* **109**, 209–228.

WAINWRIGHT, S. A. (1983). To bend a fish. In *Fish Biomechanics* (ed. P. Webb and D. Weih), pp. 68–91. New York: Praeger.

WAINWRIGHT, S. A., BIGGS, W. D., CURREY, J. D. AND GOSLINE, J. M. (1976). *Mechanical Design in Organisms*. New York: John Wiley and Sons.

WEBB, J. E. (1973). The role of the notochord in forward and reverse swimming and burrowing in the amphioxus *Branchiostoma lanceolatum*. *J. Zool., Lond.* **170**, 325–338.

WEBB, P. (1986). Kinematics of lake sturgeon, *Acipenser fulvescens*, at cruising speeds. *Can. J. Zool.* **64**, 2137–2141.

WILKINSON, L. (1989). *SYSTAT: The System for Statistics*. Evanston, IL: SYSTAT, Inc.

WOO, S. L.-Y., MOW, V. C. AND LAI, W. M. (1987). Biomechanical properties of articular cartilage. In *Handbook of Bioengineering* (ed. R. Skalak and S. Chien), pp. 4.1–4.44. New York: McGraw-Hill Book Co.